CHAPTER 1   Inflammation orchestrates differential wound healing in lizard appendages

INTRODUCTION

All organisms are engineered to repair the worn-out tissues or organs. What makes reptiles a class apart is their potential to reform a functional replica of complex tissue architecture as seen in the lizard tail (Vitt 1983; Clause and Capaldi, 2006). Adding to the already complex equation of events, is the fact that this regenerating power is immaculately confined to tail, while other appendages scar away (Alibardi, 2009; 2016). Certainly, the articulate immune response post-injury and its tissue specific vicissitudes in tail and limb, seemed to be a crucial and equally less researched field (Godwin and Rosenthal, 2014). Hence, this study is an attempt to explore the reasons behind this disparity of wound healing routes while keeping the inflammation as a focal point. Herein, we tried to unearth the technicalities of these events, to find out the hidden mechanisms and answer the big question- "How does inflammation determine the disparate course of wound healing in lizard tail and limb?

The pursuit of answers began with studying the immune system of reptiles, a branch of science, mostly side-lined by researchers. The scanty information available on reptilian immune system leaves space for a scaffold of speculations regarding the roles and function of the participating molecules (Zimmerman, 2010; 2016). Other notable features of reptiles include their largely terrestrial lifestyle, absence of metamorphosis and seasonal shift in behaviours; all having plausibly vivid impacts on immune system as well (Montali, 1988). Recently though, scientists have recognised the importance of these ectothermic amniotes' immune system evolution and last two decades have seen tremendous interest growing in this direction (Zimmerman, 2020). By far, scientists have partially worked out the similarities and differences in the immune systems of reptiles and other mammals, including humans (Montali, 1988), thus opening new avenues of research. One can fairly judge the match and mismatch of events occurring under the similar immune reactions elicited by both, reptiles and mammals. Following section throws more light on all similarities and differences marked in the physiology of immunity, inflammation and wound healing in these two classes of vertebrates, with a special insight on immune response elicited by lizards.

Immune response in Mammals and Reptiles: What we know so far

The wide range of habitats, characteristics and sizes observed in the orders of reptiles contributes to the complexity while studying their immune systems. Also, this adds to the information provided by this class on the evolutionary front, offering more conclusive inputs for researchers studying the coevolution of immune systems (Pincheira- Donoso et al., 2013). We hereby, compare and contrast all components of immune system in humans and reptiles, thus rationalising the choice of model organism and deciphering the possibilities of extrapolation of information obtained from a reptilian system on the mammalian ones.

Pathogen Recognition

The basic pathogen recognition system involving DAMPs, PAMPs and PRRs, is evolutionarily conserved in jawed vertebrates and only variation presented to these elements arises from the different types of pathogens attacking the four orders of reptiles (Priyam et al., 2016). The following signalling cascade portrays similar or higher levels of resemblance across all vertebrate classes. NF-κB pathway for instance, shows striking similarities in transcription, translocation and even regulation for both humans and crocodiles (Merchant et al., 2017). Toll like receptor (TLRs) and Myeloid differentiation primary response 88 (Myd88) based induction of IL-1β and subsequent rise in inflammation is found in both, humans and turtles (Zhou et al., 2016).

Innate Effectors

Fever is evolutionarily conserved in all vertebrate classes and enhances the defence mechanisms in organisms. What sets the reptiles apart though, is their ectothermic nature which requires them shifting to warmer places; a phenomenon known as 'behavioural fever' (Rakus et al., 2017). Multiple studies conducted on lizards have demonstrated the strong innate immune response being evoked post LPS stimulus (Uller et al., 2006; Merchant et al., 2008; Xu et al., 2016); overall serum response towards *Borrelia burgdorferi* infection was found to be more robust in lizards as compared to their mammalian counterparts (Kuo et al., 2000). Other illustrations of strong innate immunity and conserved routes of immune response come from the reports of Brazilian snakes, which elicit leukocyte migration under cytokine effects (de Carvalho et al., 2017). It is crucial to

register that recently 9 chemokines and 20 chemokine receptors in anole lizards have been identified (Nomiyama et al., 2013). In present study as well, the interaction of chemokines and wound healing machinery has been extensively studied. Inflammation, per se, can be immensely damaging for organism itself (Fullerton and Gilroy, 2016). This study revolves around impacts of inflammation on wound healing, with attempts to chart out its exact role in the latter event.

Cellular Effectors

Helper and cytotoxic T cells formulate the immune response in mammals, while the same subsets are found present in wide spectrum of reptiles (Zimmerman et al., 2010; Quesada et al., 2019). The myeloid and lymphoid cells play extensive roles in devising reptilian immunity and this study will demonstrate the alteration in their levels during various wound healing stages in a reptilian model *H. flaviviridis*. Chapter 2 focusses solely on the variable cell types contributing to the mega event of wound repair.

Humoral Effectors

Production of natural antibodies (NAbs) and B-1 cells have been recently reported in reptiles (Goessling et al., 2017; Sandmeier et al., 2018) and are shown to perform functions similar to their human counterparts. Mojave Desert tortoises and three species of neotropical snake have shown the presence of phagocytic B cells (Muñoz et al., 2014; Slama et al., 2021). NAbs on the other hand constitute the broad first line of defence system in mammals. These are also found in wide range of reptiles (Weerd et al., 2013; Judson et al., 2020) and may function to raise the bactericidal ability through opsonisation (Gray et al., 2020). The classical antibodies are also found to be conserved in all reptilian orders, though there occur some major structural variations. Also, the titre of these antibodies is highly variable amongst the reptilian orders; Crocodilians for instance have multiple subclasses of IgM, while snakes and turtles elicit single subtype (Gambón-Deza and Olivieri, 2018).

Memory

Retaining the memory of antigens previously exposed makes the clearance of pathogens efficient, if the same antigens appear again (Hoffman et al., 2016). Similar response has been identified in all classes of reptiles, nevertheless the degree and intensity of the response are variable (Hellebuyck et al., 2014; Sandmeier et al., 2017). Interestingly though, change in antibody affinity was not reported on second exposure to antigens (Zimmerman et al., 2010). It would be crucial for scientists to study the roles of innate immunity in patterning the trained immune response in case of reptiles, wherein markers of memory can become a crucial feat. Figure 1.1 illustrates the comprehensive pattern of inflammation followed in both mammals and reptiles.
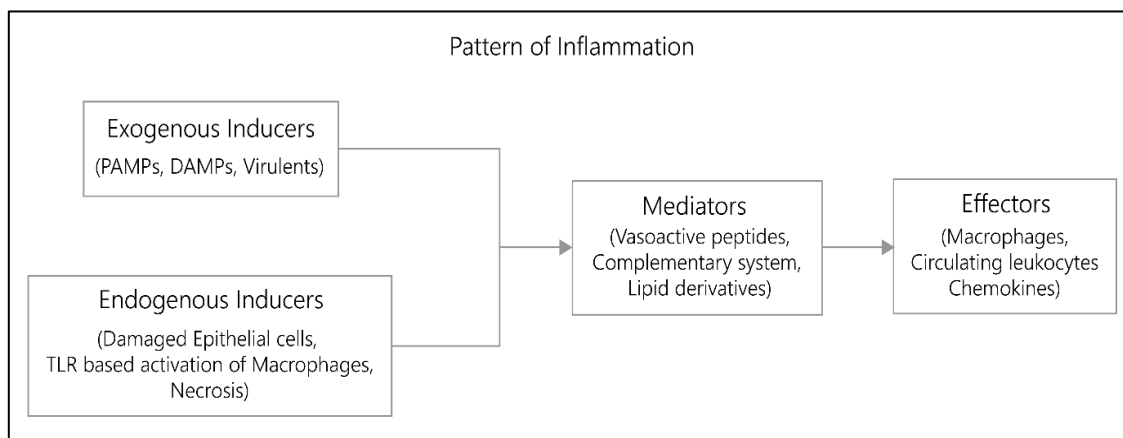

Figure 1.1: Pattern of Inflammation (Adapted from Medzhitov, 2008)

Having mentioned all the similarities and differences in the mammalian and reptilian immune response mechanisms, it still underlines the lack of specific reagents required to study the reptilian systems. This forces us to extrapolate the observations made in one system to the other. Certainly, strong evidences support the usage of reptilian model organisms for a large number of studies but job of all researchers working in this field becomes more challenging due to lack of high-end resources.

In the light of all the above-mentioned facts and all the rigorous studies performed in our lab this research idea was envisaged considering lizard, *H. flaviviridis* as a model system. Especially because it can selectively regenerate the lost tail while the other appendages (limbs) follow scarring upon amputation (Buch et al., 2017, 2018; Ranadive et al., 2018). Investigating this intriguing yet less studied model led to a lot of insight into events leading to the scar-free wound healing, a prerequisite for subsequent regeneration. Additionally,

any mechanistic details thus gained can help in understanding the causes of limited restorations, as observed in humans. As discussed in the introductory chapter, our primary goal was to assess the roles of inflammation in paving the paths of disparate wound healing.

Since inflammation touches upon multiple molecular cascades, there occur numerous controllers of this colossal event. The proportion and outreach of the inflammatory response is scaled based on the chosen regulatory pathway (Schmid-Schönbein, 2006). One such mediatory regulator of inflammation, named as cyclooxygenase resides at the core of present study. Immunomodulation carried out by the members of this family (COX-1 and COX-2) are discussed in great detail, further in this chapter and primarily illustrated in figure 1.2. Technically, the mediators are chosen based on the type, location and extent of injury. These mediators also deploy few additional molecules to efficiently counter the pathogenic influx at the site of injury (Hata and Breyer, 2004; Li et al., 2015).
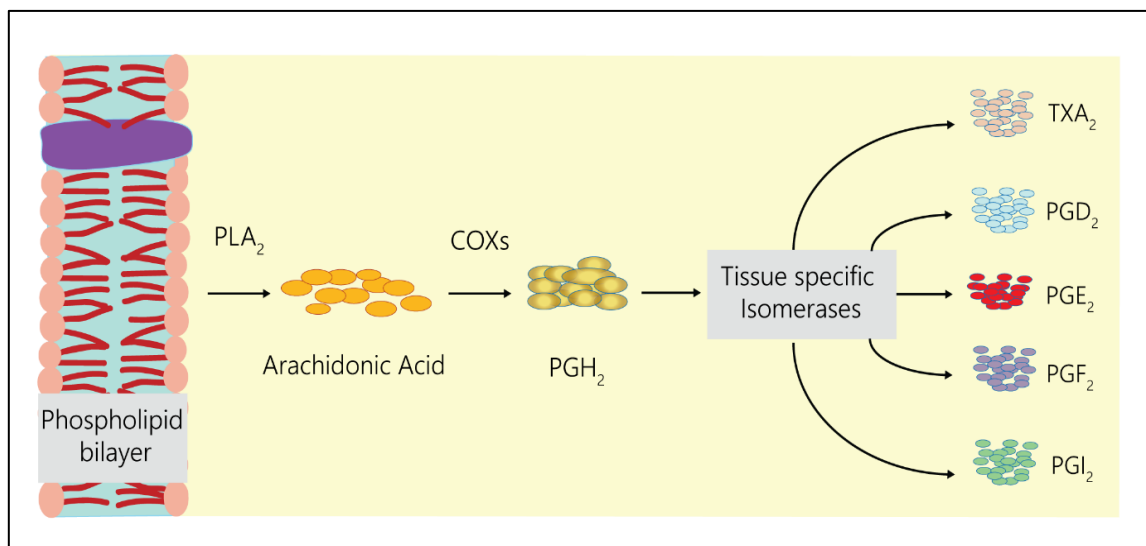

Figure 1.2: COX-Prostaglandin pathway

COX and Prostaglandins: Incite and Influence Inflammation

Of all the initiator molecules causing inflammation, lipids and their derivatives are considered to be conserved across the animal clans. Specific enzymatic reactions and stringently regulated pathways control the release and function of these mediators (Langenbach et al., 1995; Smyth et al., 2009). Prostaglandins (PGs) and Thromboxanes (TXs) constitute one of the most important lipid group of Prostanoids, that performs significant functions towards cell homeostasis and repair (Bos et al., 2004). Precursor of

prostanoid formation is Arachidonic acid (AA), which is released from the phospholipid bilayer of cell membrane under the catalytic function of phospholipases (PLs) (Bos et al., 2004; Ricciotti and FitzGerald, 2011). The released AAs are then worked upon by COXs, which are crucial for normal and stabilised physiology of the cell. COXs exist predominantly in two isoforms COX-1 and COX-2 (Dubois et al., 1998); the latest one discovered. COX-3, is a splice variant of COX-1 (Flower, 2003).

On account of successful homeostatic functions, COX-1 stands responsible, rather inevitable. Its absence or inhibition has been reported to cause deleterious effects on intestinal lumen and kidney function (Simmons et al., 2004). COX-2 on the other hand, is the prevalent inducible form, titre of which rises in the cells under stimuli such as injury, infection and inflammation (Seibert et al, 1994; Kuwano et al., 2004; Simmons et al., 2004). In the present study as well, influence of COX on inflammation and wound healing has been recorded while following the track of other immune modulators. Activity of COX isoforms (both COX-1 and COX-2), generates Prostaglandin G_2 (PGG_2), which gets reduced further to form PGH_2. Based on the functional variations in different tissues, specific isomerases catalyse the conversion of PGH_2 into different isomers of prostanoids namely PGE_2, PGI_2 PGD_2, $PGF_{2\alpha}$ and TXs (Funk et al., 2001; Ricciotti and FitzGerald, 2011; Yao and Narumiya, 2019).

All prostanoids are produced ubiquitously in all cell types, though their expression alters dramatically during inflammation (Ricciotti and FitzGerald, 2011). Once again, the enzymes acting site specifically on PGH_2 is responsible for the variable concentrations of all prostaglandins. PGE_2 plays the most crucial role in mediating inflammation as it signals leukocyte migration and cytokine recruitment at the site of injury as well (Harris et al., 2002). Microsomal PGE synthase-1 (mPGES-1), mPGES-2, and cytosolic PGE synthase (cPGES) are the three PGE synthase isoforms, of which the first one takes up the charge under inflammatory cues, while the latter two are more of housekeeping in function (Gudis et al., 2005).

Every prostaglandin instructs and deploys multiple signalling pathways in a ligand-receptor action (Copeland et al., 1994; Harris et al., 2002). PGE_2 invokes all its downstream operations through a family of receptor isoforms named as Prostaglandin E receptors- EP1, EP2, EP3 and EP4 (Sugimoto and Narumiya, 2007). Based on chosen receptor, the course of action varies

vastly and provide vital signals for orchestrating and fine-tuning inflammation (Kawahara et al., 2015). Hence, the present study was drafted to observe and follow the path of action of COX-2 derived PGE_2-EP receptor signalling in driving inflammation and wound healing of lizard appendages.

In structural terms, EP receptors are PGE_2 specific G protein coupled receptors (GPCRs) (Sugimoto and Narumiya, 2007). It is crucial to note that EP receptors in coherence with the upstream instructions lead to either proinflammatory or antiinflammatory outcomes, thus recruiting respective cells and cytokines at the site of healing (Akaogi et al., 2004).
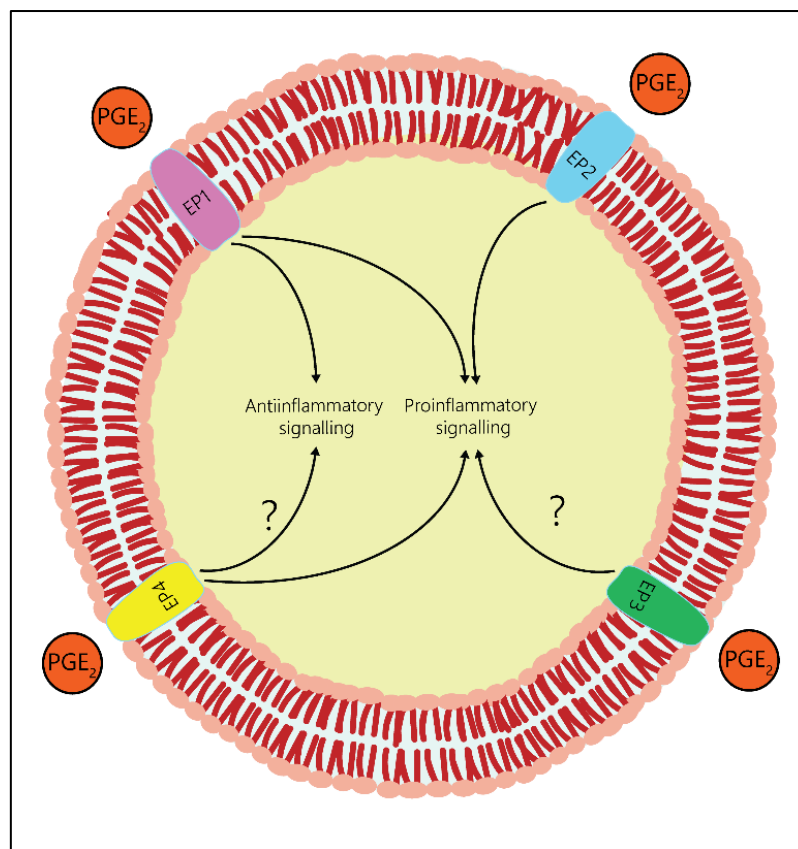

Figure 1.3: PGE_2-EP based inflammation regulation

The cryptic side of PGE_2 has now been revealed, which shows the antiinflammatory action of this prostanoid, contrasting with its well established proinflammatory character. Research groups such as Coulombe and coworkers (2015), while researching influenza virus in the infected systems have highlighted tissue specific and receptor mediated antiinflammatory roles of PGE_2. Serezani group's findings pertaining to bacterial killing by macrophages (2007) and many others have recorded similar features of PGE_2, which have promoted wound healing or rather rescued the systems from entering chronic

inflammation (Yao and Narumiya, 2019). As shown in figure 1.3, both pro and antiinflammatory actions of PGE_2 are again relayed through the EP receptors in a concentration dependent fashion recruiting a cohort of respective interleukins to either promote inflammation or curb it (North et al., 2007; Brenneis et al., 2011; Kalinski, 2012).

Resolution of inflammation is a part of the bigger frame, where repair method designates the fate of the wounded region (Eming et al., 2007; Rosique et al., 2015). Intriguingly, the revamp routes are not conserved evolutionarily and do not necessarily improve with the growing complexity of the organisms across the cladogram, as we observed in the earlier sections. Reptiles, by and large have possessed the capacity of restoring lost tissues, what is peculiar about Northern House Gecko is the stringent bias followed in the healing mechanisms deployed by its appendages (Sharma and Suresh, 2008; Alibardi, 2009). Also, the time taken for the entire healing process to unfold and the visible morphological changes across the time scale are prominently contrasting to each other in tail (Figure 1.4) and limbs (Figure 1.5).
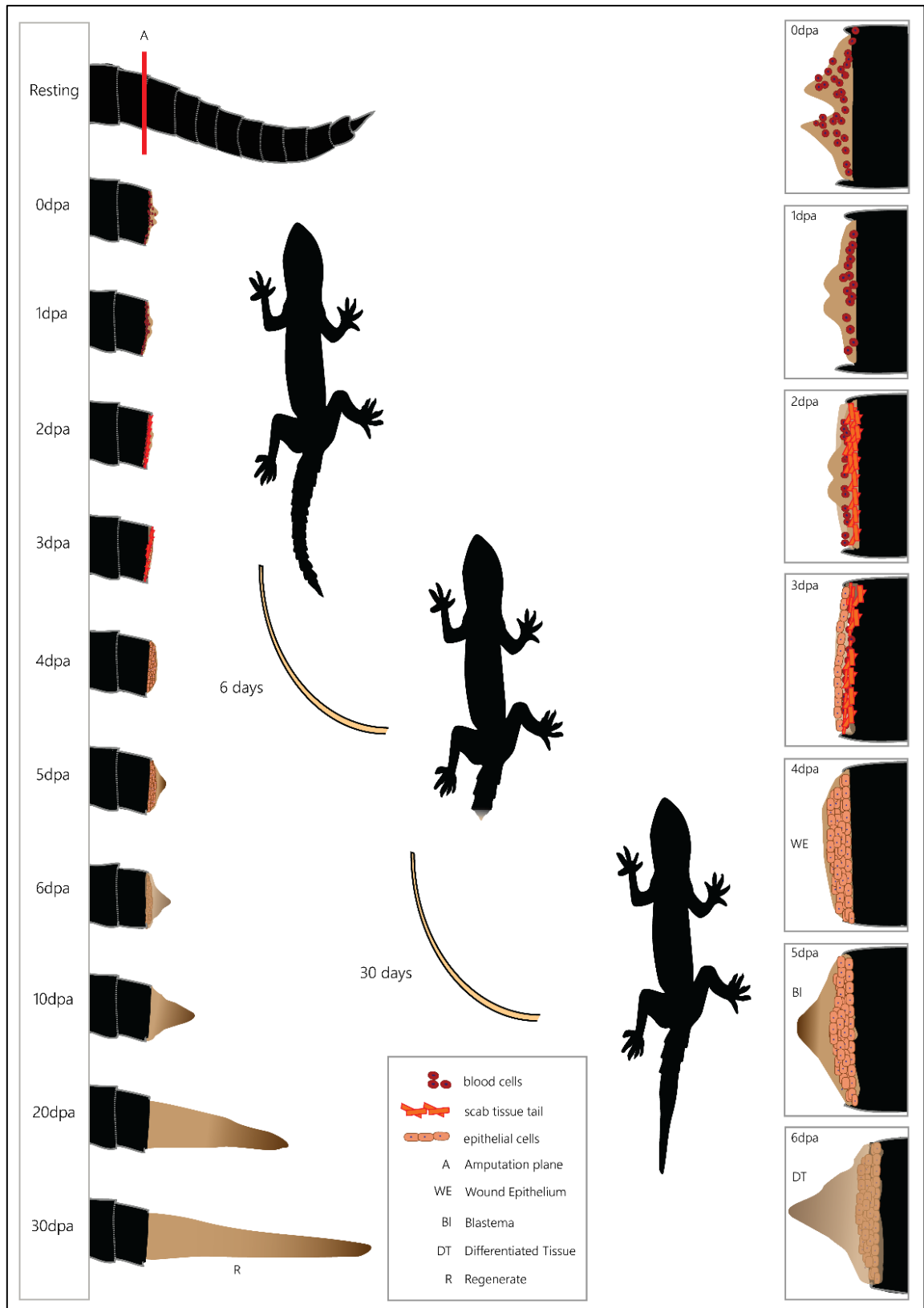
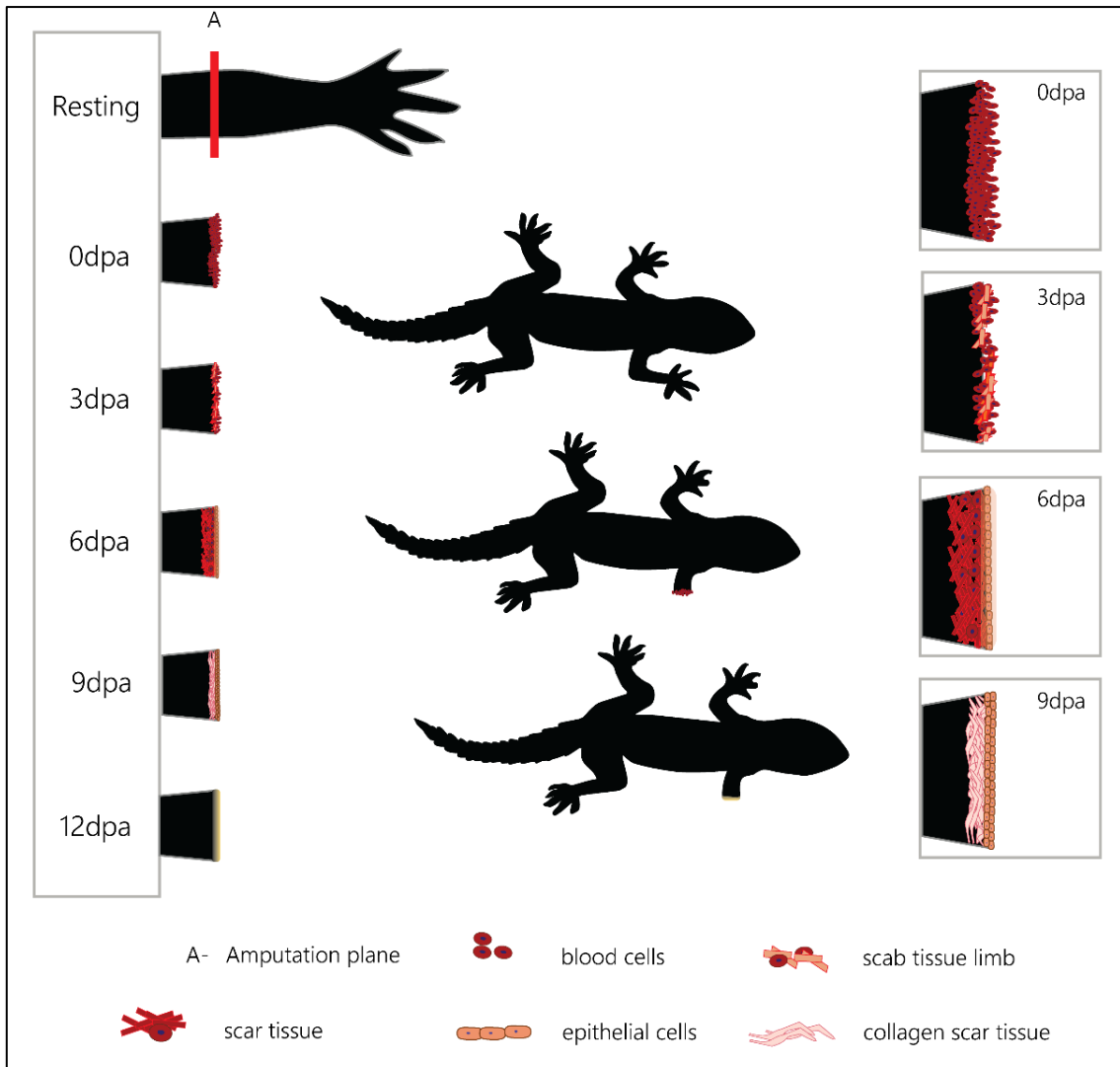Figure 1.4: Wound healing in lizard tail

Figure 1.5: Wound healing in lizard limb

Hence inflammation was chosen for further investigation as being the first step, it would plausibly direct the differential wound healing regimen and create organ specific micro environment, either leading to scar-free 'super healing' or scar formation. Additionally, the mechanistic details thus gained can help in understanding the causes of limited restorations, as observed in humans.

In an effort to unearth the basic mechanisms, after a series of preliminary screening, the regulators of inflammation like COX-2, PGE_2, its receptors (EP2 and EP4) followed by inflammatory mediators, namely- iNOS, TNF-α, IL-6, IL-10, IL-17, and IL-22, which function in coordination with COX-2, were considered for this study. The specific choice of COX-2 as a mediator of interest was made in the light of previous study from our lab, which highlights its role in achieving epithelialisation and proliferation in the regenerating tail of *H.*

flaviviridis via Wnt/β-Catenin pathway (Buch et al., 2017). In few other studies, role of COX-2 derived PGE_2 has been proven in initiation and progression of regeneration in lizard tail (Sharma and Suresh, 2008; Buch et al., 2017). In the present report, 'COX-2' has been used, uniformly, instead of the gene name-PTGS-2, to avoid confusion. The detailed architecture of the healing tail and limb have been elaborately reported by Alibardi (2014) and Vitulo et al. (2017), using immunohistochemistry. The novel aspect observed in this study is the appendage-specific action of inflammatory mediators, which leads to early resolution or prolonged stay of inflammation in the healing microenvironment, which plausibly causes either a scar-free wound healing as a forerunner of regenerative outgrowth in tail or forms a permanent scar tissue in the limb.

MATERIALS AND METHODS

Hemidactylus flaviviridis (Northern House Gecko), both male and female, were caught from a nearby locality and caged in wooden chambers. Housing conditions were maintained as reported by Buch and colleagues (2017). Details of protocol are discussed in Materials and Methods section.

For investigating the molecular events of inflammation in the appendages, the animals were randomly categorised into two main groups, namely tail and limb. These groups were further divided in various sub-groups based on the stage of the healing process to be targeted. For tail, 0, 1, 2, 3, and 4dpa (days post-amputation) and for limb, 0, 3, 6 and 9dpa were considered for the study, as these highlight the haemostasis and granulation along with the increased inflammation, culminating in scab formation, followed by appearance of wound epithelium. Detailed rationale and experimental protocols are as discussed in Materials and Methods.

Morphometry, COX activity assay, PGE_2 estimation assay as well as COX-2 localisation through Immunohistochemistry were performed on the samples collected from control and treated groups. In order to check the protein and gene expression of cytokines, Western blot and Quantitative real-time PCR analysis were performed. Details of the protocol followed along with the methods used are mentioned in Materials and Methods section along with the primers used for gene expression analysis are mentioned in Table 1.

RESULTS

Morphological observations

The periodic changes occurring during the diverse healing frames of tail and limb were recorded from both the groups. Pattern of repair is conspicuously different and the morphological panel created here just provides the supportive evidences for the same (Figure 1.6).

Temporal variation in the activity of COX-2 in the healing tail and limb

COX activity at various stages of scar-free and scarred wound healing were compared in tail (Figure 1.7A) and limb (Figure 1.7B), respectively. In the tail, the activity of COX-2 showed significant increase at all the wound healing stages of tail, when compared to 0dpa (Figure 1.7A). Similarly, in limb, COX-2 levels increased significantly at 3dpa, 6dpa and 9dpa as compared to with 0dpa (Figure 1.7B). Since the COX-2 activity levels were found to be high in both the appendages during their respective healing stages, a major mediator of inflammation downstream of COX-2, which controls the resultant modulations, namely PGE_2 (Prisk and Huard, 2003; Parmar et al., 2021; Verma et al., 2021) was targeted.

PGE_2 level in the healing appendages

Prostaglandin E_2 is a pivotal contributor to inflammation, synthesis of which is initiated by the injury-induced activation of the enzyme COX-2 (Korbecki et al., 2014). Levels of PGE_2 were analysed at the selected time windows in both tail and limb. An increase in PGE_2 level was observed in tail tissue from 1dpa till 4dpa when compared to the resting stage (Figure 1.8A). On the other hand, in limb, a downward trend was observed in the level of PGE_2 starting from 3dpa till 9dpa, all significantly lower as compared to 0dpa (Figure 1.8B). The readable observation was the well-pronounced reduction observed in the PGE_2 level in limb as opposed to tail.

Distribution pattern of COX-2 in the healing appendages

COX-2 was localised in the tissues collected at destined time points from both the appendages and the subsequent microscopic analysis vividly portrayed the temporal changes in its site of expression. In tail tissue, initially at 0dpa, a faint expression of COX-

2 at the site of autotomy was observed (Figure 1.9A). Although, in the following stages of wound healing in tail, COX-2 was found to be localised differentially. COX-2 was localised near spinal cord at 1dpa in tail tissue (Figure 1.9B) whereas its expression was observed in the intermediate region between epidermis and spinal cord at 2dpa (Figure 1.9C). In 4dpa tissue, COX-2 was seen just under the epithelial ectoderm of tail (Figure 1.9D). In case of limb, visible expression of COX-2 in the tissue section, at the site of amputation in 0dpa stage was observed (Figure 1.9E). At 3dpa, COX-2 was localised over the injured surface of humerus immediately beneath the clot (Figure 1.9F). At 6dpa, COX-2 was localised in the chondrocytes covering the humerus bone as well as in the newly formed epithelial layer (Figure 1.9G). A remarkable difference was observed in the site of COX-2 expression in both tissues (tail and limb), wherein the area of its localisation changed temporally. For instance, COX-2 localisation peculiarly shifted from the proximal region of progressive epithelium covering the amputated limb in 6dpa (Figure 1.9G) to closer to the dermal layer by 9dpa, where the persistent scar is formed (Figure 1.9H). The schematic representation is shown near the respective figures, to explain the exact location of COX-2, found to be temporally changing, across the healing frames of the appendages (Figure 1.9). The tissue regions and cell types identified here are based on the previously reported histological details of both the appendages, in our lab (Ranadive et al., 2018).

Protein expression pattern of the inflammatory mediators in healing appendages

Protein expression was checked for the major regulators of inflammation in both tail and limb. COX-2 protein levels in the tail went up for 1dpa, 2dpa, 3dpa and 4dpa in comparison to 0dpa (Figure 1.10A; Table 2A). In limb tissue, the expression noticeably increased at 3dpa, but maintained at the same level at 6dpa as compared to resting stage. At 9dpa, COX-2 protein levels remained elevated as compared to 0dpa (Figure 1.10B; Table 2B). The protein levels of EP2 receptor were found to be constantly decreasing in tail whereas in limb its levels were significantly increased from 0dpa till 9dpa. Simultaneously, protein expression of EP4 receptor was found to be increased throughout the wound healing stages of tail in comparison to resting stage (Figure 1.10A; Table 2A). However, striking difference in the level of EP4 was observed in scarring limb wherein its level went down significantly from 0dpa and continued to do so till 9dpa (Figure 1.10B; Table 2B).

Simultaneously, few pivotal proinflammatory mediators were checked for their expression, namely iNOS, TNF-α, IL-6, and IL-17. Expression levels of iNOS and TNF-α in tail were found to be reducing from 2dpa to 4dpa stage when compared to 0dpa (Figure 1.10A; Table 2A). On the contrary, the protein levels of iNOS and TNF-α were found to be increased during scarring in limb when compared to 0dpa (Figure 1.10B; Table 2B). Expression level of one of the principal antiinflammatory mediator IL-10, was also monitored and was found to be successively increasing from 0dpa to 4dpa in tail (Figure 1.10A; Table 2A), while its levels stooped significantly in limb after 3dpa and remained low till 9dpa stage (Figure 1.10B; Table 2B). Protein level of IL-6 in tail was decreased starting from 1dpa till 4dpa in tail whereas in limb it was found to be reduced at 3dpa however 6dpa onwards the level increased till 9dpa in limb (Figure 1.10A-B; Table 2A-B). IL-17 protein levels were decreased noticeably from 1dpa to 4dpa in comparison to 0dpa in tail (Figure 1.10A; Table 2A). In case of limb, IL-17 protein levels were found to be decreased significantly from 0dpa to 3dpa, followed by a sudden rise noted for 6dpa and 9dpa (Figure 1.10B; Table 2B). IL-22 elicited a riveting result wherein, its protein expression increased from resting stage till 4dpa in tail. IL-22 showed marked decrease in the expression at 3dpa stage of healing limb but then gradually elevated at 6dpa followed by remarkable rise at 9dpa, when compared with 0dpa (Figure 1.10A-B; Table 2A-B).

Gene expression pattern of inflammatory mediators in healing appendages

Quantitative real-time PCR was employed to further validate the expression status of various regulatory molecules at transcript level, which organise the entire inflammatory response in these two varied appendages. These molecules were majorly considered for their distinct roles, either supporting or opposing inflammation. Both tail and limb groups showed major alterations in the expression of these molecules. The genes considered were, COX-2, EP2, EP4, iNOS, TNF-α, IL-10, IL-6, IL-17 and IL-22 (Figure 1.11 and 1.12; Table 3A and B). COX-2 is known to be upregulated under the effect of an injury, so was observed here, wherein significant elevation was observed in its transcript-level expression, under the impact of induced autotomy in the tail. Results showed a striking rise in COX-2 expression from 0 to 3dpa by almost 16-fold which then remained 8-fold at 4dpa in comparison to 0dpa for the tail (Figure 1.11; Table 3A). The subjects of the limb group also showed a progressive elevation in COX-2 mRNA from 0 to 9dpa (Figure 1.12; Table 3B).

Additionally, the level of EP2, a member of the PGE$_2$ receptor family, was checked, which showed noticeable variation in expression. The EP2 gene expression was in concurrence with its protein expression data wherein the levels increased till 3dpa followed by reduction at 4dpa decreased throughout the course of healing in tail (Figure 1.11; Table 3A) and were upregulated in scarring limb (Figure 1.12; Table 3B). Another PGE$_2$ receptor, EP4 was checked in tail and it elicited rise in gene expression at 1dpa and remained elevated till 4dpa, when compared to 0dpa (Figure 1.11; Table 3A). On the limb front EP4, it decreased significantly across 3dpa, 6dpa and 9dpa (Figure 1.12; Table 3B).

Various proinflammatory mediators, boosting the course of inflammation were checked, namely-iNOS, TNF-α and IL-6, for their temporal gene expression pattern. All these three genes showed prominent reduction from 1dpa till 4dpa as compared to 0dpa during lizard tail regeneration (Figure 1.11; Table 3A). However, during limb healing, iNOS, TNF-α and IL-6 transcript levels were upregulated remarkably in comparison to 0dpa (Figure 1.12; Table 3B). Thus, iNOS, TNF-α, and IL-6, all showed progressive reduction in expression during the course of wound healing in tail, while the antiinflammatory mediators IL-10 showed increase of expression (Figure 1.11; Table 3A). Herein, conspicuous rise in its gene expression was recorded from 1dpa onwards, which progressed across 2, 3 and 4dpa stages to increase by 13-folds at the terminal time point, as compared to the resting one (Figure 1.11; Table 3A). On the contrary, a significant reduction in its expression was observed at the 6dpa of limb, after a marked elevation at 3dpa, followed by further decrease at the final time point of 9dpa (Figure 1.12; Table 3B). Thus, subjects of the limb group, showed exact contrast, to the tail group, with respect to the trend of gene expression, as the proinflammatory mediators displayed a prominent rise while the antiinflammatory molecule elicited evident reduction (Figure 1.11 and 1.12; Table 3A and B).

Apart from these genes, we found specific changes in the status of IL-17 and IL-22 gene expressions. During our study we found IL-17, to be reducing in an ordered fashion, in the tail tissues (Figure 1.11; Table 3A). Initially, it rose from 0 to 2dpa only to be reduced by 3dpa, also staying down by the end of 4dpa. In such an environment, IL-22 portrayed a constructive character and supported the fast-healing process of the tail, possibly because its levels also increased till 2dpa as compared to the resting stage, followed by peculiar heightened numbers at 3dpa, which only reduced significantly at the last time point studied, i.e., 4dpa (Figure 1.11; Table 3A).

On the other hand, in the case of the limb, IL-17 showed a major reduction in gene expression at 3dpa followed by a significant hike at 6dpa, which reduced again at 9dpa, as compared to 0dpa. Congruently, IL-22 transcripts too reduced remarkably at 3dpa followed by a sudden hike at 6dpa, while it returned to near basal level at 9dpa, when compared to the resting stage (Figure 1.12; Table 3B).

DISCUSSION

This study is a diligent attempt to highlight the involvement and impact of inflammation on wound healing of lizard appendages, viz., tail and limb. As per our prevalent knowledge of over many decades now, cyclooxygenase, is a family of enzymes, which regulates and fine-tunes multiple developmental programmes like cell survival, proliferation and migration (Lu et al., 1995; Dubois et al., 1998; Simmons et al., 2004; Liou et al., 2007). The results obtained here suggest that COX-2, an inducible isoform of COX, plausibly modulates inflammation through varied PGE_2-EP receptor signalling, wherein specific interleukins are recruited at the site of repair.

COX-2 activity elevated from 2dpa onwards in lizard tail, while in limb it was relatively high and increased progressively at the following time points. As COX-2 belongs to the family of early response genes and is strongly induced by mitogenic and proinflammatory stimuli (Lasa et al., 2000), checking its protein expression and activity was a mandate. In concurrence to its hiked activity, COX-2 protein and gene levels were also found to be elevated till the 3dpa stage in tail. This suggests participation of COX-2 in modulating early inflammation, which got reduced at 4dpa, during proliferation and epithelialisation. On the contrary, in limbs COX-2 gene expression increased from the basal level till the terminal time point of 9dpa. This suggests mRNA stabilisation in limb tissue, due to elevated proinflammatory interleukins as found by Kang and colleagues in human bones, macrophages and granulosa cells (Kang et al., 2007).

Further, COX-2 activity forms PGE_2 as an early response gene product, boosted by proinflammatory cytokines, governing its transcriptional and post-transcriptional levels (Kang et al., 2007). PGE_2 expression followed a trend of COX-2 activity in tail, while in limb, it showed significant decrease after 3dpa, until 9dpa. Interestingly, the basal level of PGE_2 in limb (0dpa) is higher than the terminal time point for tail (9dpa). This disparity

could be a function of COX-2 driving multiple signalling pathways in various tissues in a context specific manner (Dubois et al., 1998; Simmons et al., 2004; Tsatsanis et al., 2006). Also, other tissue specific inflammation curbing prostanoids might participate to cause early resolution (Bos et al., 2004; Korbecki et al., 2014) and resultant super healing in tail, while contrasting results are observed in limb (Khaire et al., 2021) Meanwhile, a complete profiling of all prostanoids participating in these events, would explain their roles in regulation of inflammation.

Aoki and Narumiya (2017), have established that PGE_2 and its interaction with the downstream receptor (EP1-4), determines the course of inflammation in the healing tissue. Also, the intracellular messengers such as, cyclic adenosine mono phosphate (cAMP) and phosphorylated-cAMP response element binding protein (phospho-CREB) function under the EP2 and EP4 activation to cause a hike in gene and protein levels of proinflammatory cytokines, which then support inflammation by regulating both, its manifestation and resolution (Smith, 1992; Bos et al., 2004).

Present results suggest a similar tissue specific PGE_2-EP receptor action, as in tail, along with EP2, IL-6, a major proinflammatory mediator got alleviated. On the other hand, in limb, EP2 levels elevated for both protein and gene expression, along with steady rise in the levels of the major proinflammatory mediators such as iNOS, TNF-α and IL-6. The correlation of the EP2 receptors with the downstream proinflammatory mediators has been reported earlier too (Hinson et al., 1996; Aoki and Narumiya, 2017). On the contrary, the antiinflammatory action of EP4 has also been reported in a wide array of systems (Heffron et al., 2021; Joshi et al., 2021; Yasui-Kato et al., 2020). In the present model too, this evident contrast in the EP2-EP4 expression pattern could be the primary reason for the exquisite dissimilarity in the status of inflammation. This contrasting appearance and action of the two receptors, might recruit differential cluster of either anti or proinflammatory mediators at the site of wound healing in tail and limb, respectively.

Major proinflammatory mediators, iNOS, TNF-α, IL-6, etc work in congruence to promote the tissue-specific inflammation at the site of injury, while they function as per the COX-2 mediated PGE_2 expression and its binding with the downstream EP receptors (Hinson et al., 1996; Harris et al., 2002). It is the stark difference in the levels of these regulators (PGE_2

and EP receptors) and their periodic expression, which possibly lays the foundation of biased wound healing in both the appendages.

TNF-α is a well-established proinflammatory mediator (Lawrence et al., 2009), that functions in coherence with PGE_2 and recruits other inflammation boosting interleukins such as IL-6 (Hinson et al., 1996) and rising expression of this prostaglandin as well (Harris et al., 2002). In the present study, TNF-α and IL-6 show distinct decline in the gene and protein expression in tail, overlapping haemostasis and epithelialisation stages of wound healing. These levels further stoop during the proliferative phase by the fourth day of amputation. On the contrary, in limbs, TNF-α and IL-6 showed continuous rise till 9dpa, confirming the prolonged high levels of inflammation in the microenvironment. Along with these proinflammatory cytokines, their antiinflammatory counterparts are also recruited, which form the necessary balance for the successful tissue repair (Renz et al., 1988; Hinson et al., 1996; Ricciotti and FitzGerald, 2011). In present results, gene and protein levels of a major antiinflammatory mediator IL-10 spiked significantly in the tail but was found to be reduced during the healing course in limb. This substantial disparity in expression could be responsible for early and delayed epithelialisation found in tail (Figure 1.9B-C) and limb (Figure 1.9F-H), respectively. Peranteau and colleagues (2008), have reported the positive effect of IL-10 overexpression in an adult mice model of regeneration. The collaborative functions of the EP2 and EP4 receptors, which recruit and regulate these cytokines during wound healing (Hinson et al., 1996; Portanova et al., 1996; Harris et al., 2002; Harizi et al., 2003), could be responsible for its differential outcome.

However, with respect to the transcript and protein, the most striking observations were made for IL-17 and IL-22. Through studies on IL-17 KO mice, Yang and co-workers (2008) have proven its major role in inducing inflammation that positively leads to tissue remodelling. Remarkably, this is for the first time that its role is being revealed in the animal model of appendage regeneration. Its differential behaviour is studied here in two contrasting tissues, which have taken opposite paths of wound healing. IL-17 showed significant reduction in gene expression traversing all the time points, for tail group, after the early inflammation (2dpa). This supports the idea that reduction of chief proinflammatory mediators cause an overall decline of inflammation at tissue level in tail and promote regeneration supportive wound healing (Figure 1.9A-D). As opined by Veldhoen and group (2006), reduction in IL-17 expression can be a coherent effect of

another regulatory mediator like IL-6, which has shown a major decline in tail. It could even be due to the specific signalling dictated by the EP receptors (Hinson et al., 1996). Nevertheless, in limb tissue, IL-17 was elevated, except at the time when scar formation and collagen deposition started at the site of healing (Figure 1.9H). This disparity could be because by the end of scab formation, a permanent scar is constructed via collagen deposition and recruitment of fibroblast cells (Ranadive et al., 2018), while the tissue inflammation recedes to enhance the former process. Discovering this novel participation of IL-17 in the regeneration model recommends further investigation, where the performance of this cardinal inflammatory mediator can be explored.

IL-22, in the tail tissue showed well pronounced increase in its transcripts from 1dpa till 3dpa, after which its level reduced significantly by 4dpa. This ensures its participation in early epithelialisation, as achieved in tail. IL-22 elicits a protective role, when combined with IL-17, which specifically induces anti-microbial peptides in human keratinocytes (Sabat et al., 2013). Moreover, reduction of IL-17 could possibly influence the levels of IL-22 as observed in few other models like human T-cells (Veldhoen et al., 2006). This could be majorly because it is a cytokine of IL-10 superfamily, levels of which plunge under excessive inflammation (Zheng et al., 2007), as observed here in case of limb tissues. Herein, IL-22 followed the trend of IL-17, with noticeable rise in gene expression at the time of scab formation in limb tissue, in congruence with other proinflammatory mediators like IL-6, TNF-α, iNOS and IL-17. It is thus proved that IL-22 plays its part in repairing the wound in the two appendages, in synergy with IL-17 and reconstructs the framework for scar-free healing in tail (Figure 1.9D), however, it supports scar formation (Figure 1.9H) under the prolonged inflammatory response in limb.

Overall, this is an inquisitive effort to deduce the crosstalk between inflammation and the colossal course of events leading to differential wound healing in lizard. These findings reinforce the concept that inflammation can hinder the restoration proceedings if its elevated levels remain persistent for a longer duration of time (Mescher et al., 2013). The COX-2 mediated PGE_2 might play a pivotal role in symphonising the entire event of the inflammation as it operates and directs the interleukin function at the site of tissue repair. COX-2-PGE_2-EP receptor cascade plausibly governs both, restoration of lost tissue via scar-free wound healing or a permanent scar formation at the locale of injury. Hence, this

study again establishes the dual role of inflammation in boosting and banishing the regenerative process.

CONCLUSION

COX-2 derived PGE_2 might alter the expression of inflammatory mediators depending upon the receptor action downstream. The mediators of inflammation, both supporting and inhibiting its progression, are recruited at the site of healing in an appendage specific fashion. Reduction in inflammation due to PGE_2-EP4 dependant rise in IL-10 causes scar-free repair in the tail, supporting regenerative outcome. However, in limb, elevated levels of proinflammatory mediators based on PGE_2-EP2 action support scar formation instead. Illustrating the contribution of these mediators here would help us further explore the course of action deployed by these molecules in future studies. The findings and conclusion of this chapter are summarised in figure 1.13.
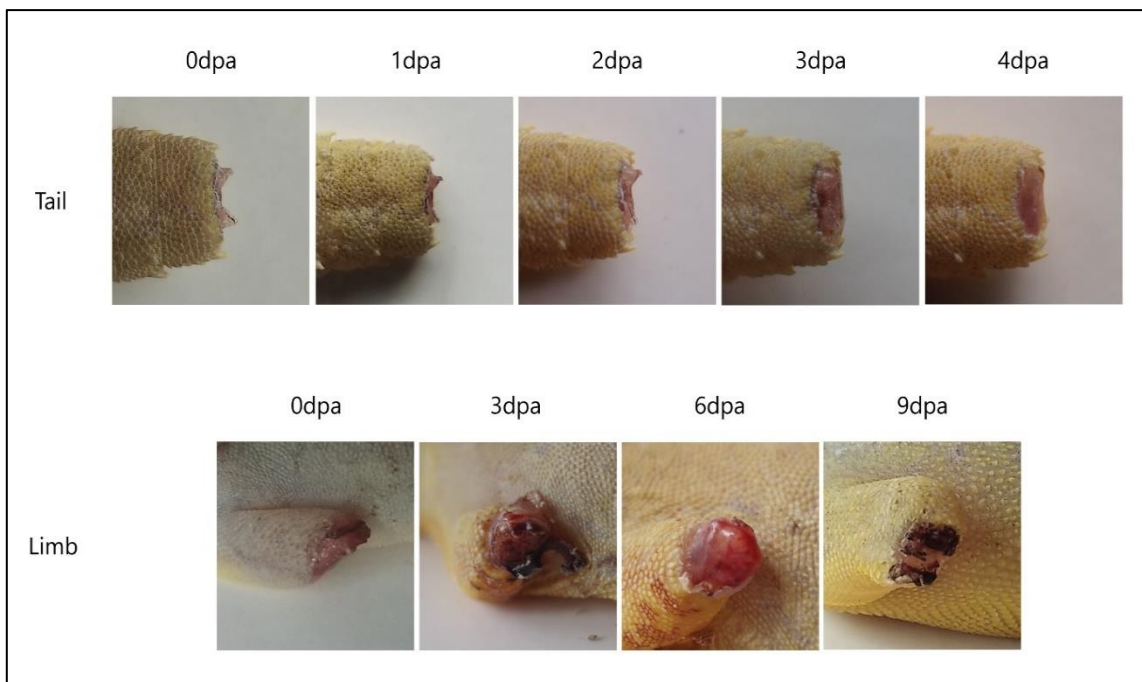

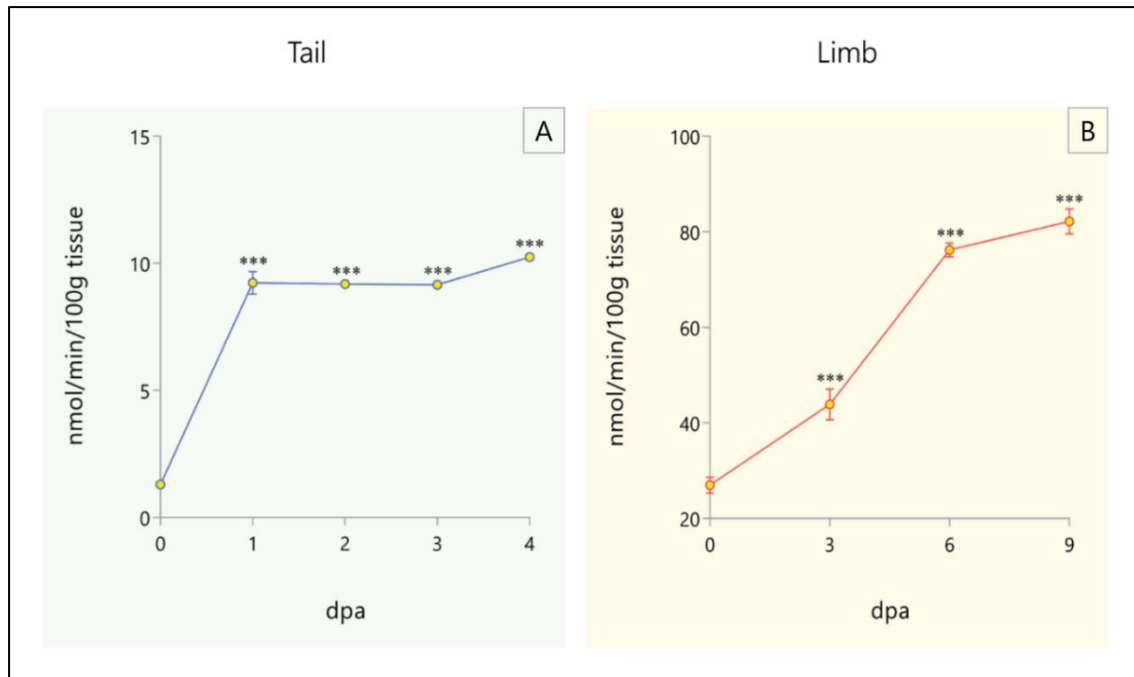Figure 1.6: Morphological changes in the healing tail and limb

Figure 1.7: COX-2 activity analysis

A: COX-2 activity in healing tail; B: COX-2 activity in healing limb. ***$p \leq 0.001$; n = 6.
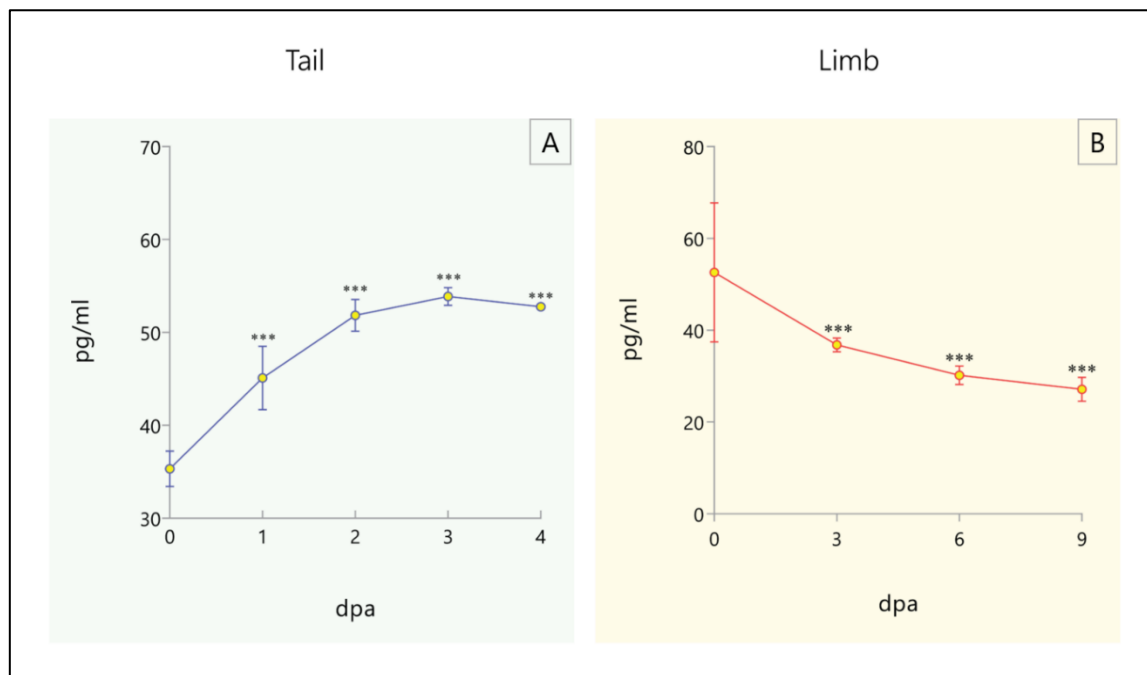
Figure 1.8: PGE$_2$ estimation assay

A: COX-2 activity in healing tail; B: COX-2 activity in healing limb. ***$p \leq 0.001$; n = 6.
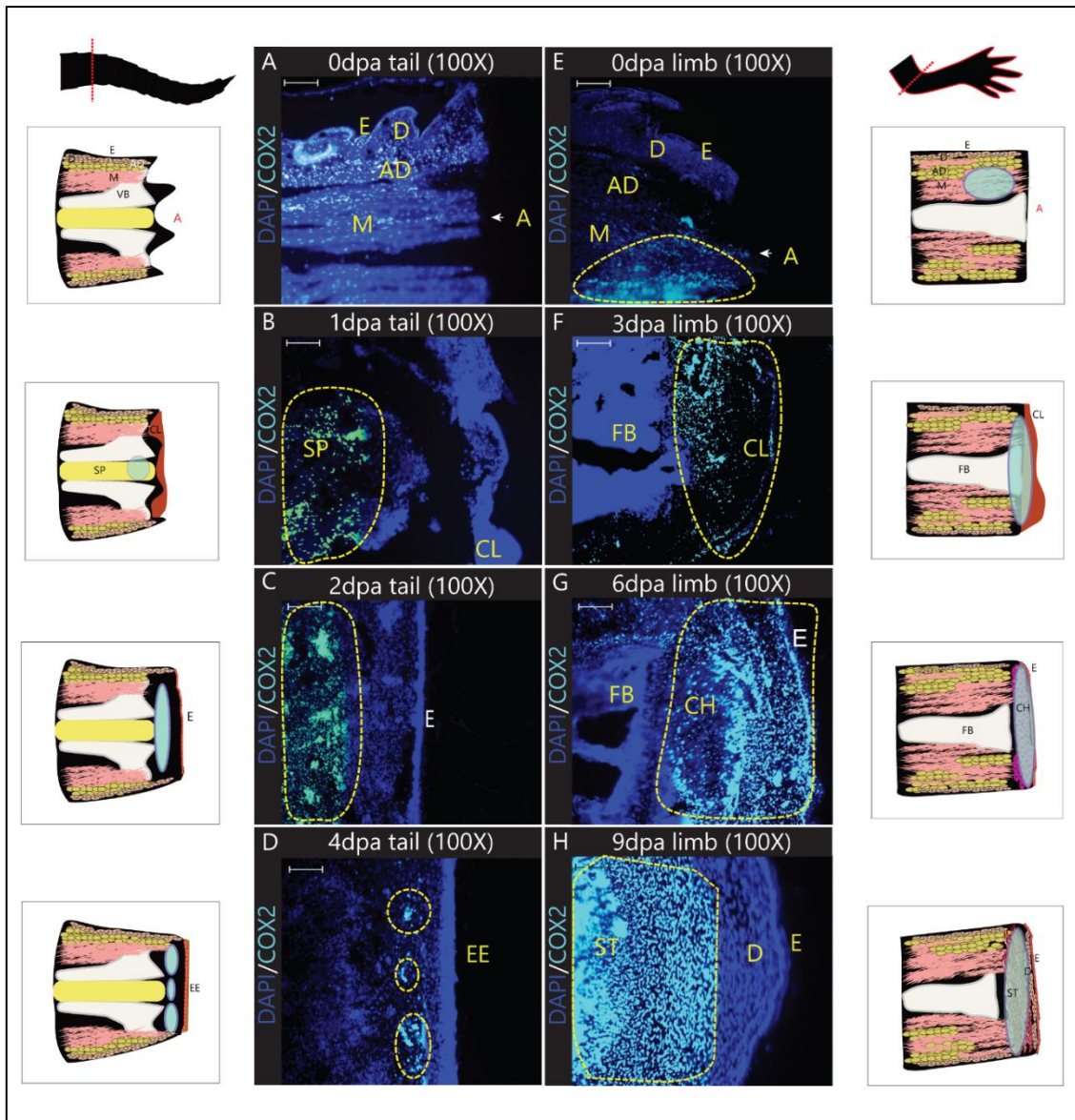
Figure 1.9: COX-2 localisation in limb and tail

Immunohistochemical localisation of COX-2: Altering intensity and sites of COX-2 localisation in the healing Tail (A-D) and Limb (E-H). Yellow dotted line depicts the site of COX-2 expression in both the tissues. A-Amputation plane; AD-Adipocyte region; EE-Epithelial Ectoderm; CH-Chondrocyte region; CL-Clot; D-Dermal region, E-Epidermal region; FB- Femur Bone; M-Muscles; SP-Spinal cord region; ST-Scar tissue; VB-Vertebral Bone. Scale bar = 200 µm. The schematic representation explains amputation plane and points out the location of COX-2 in the tissue sections, shown in cyan colour.
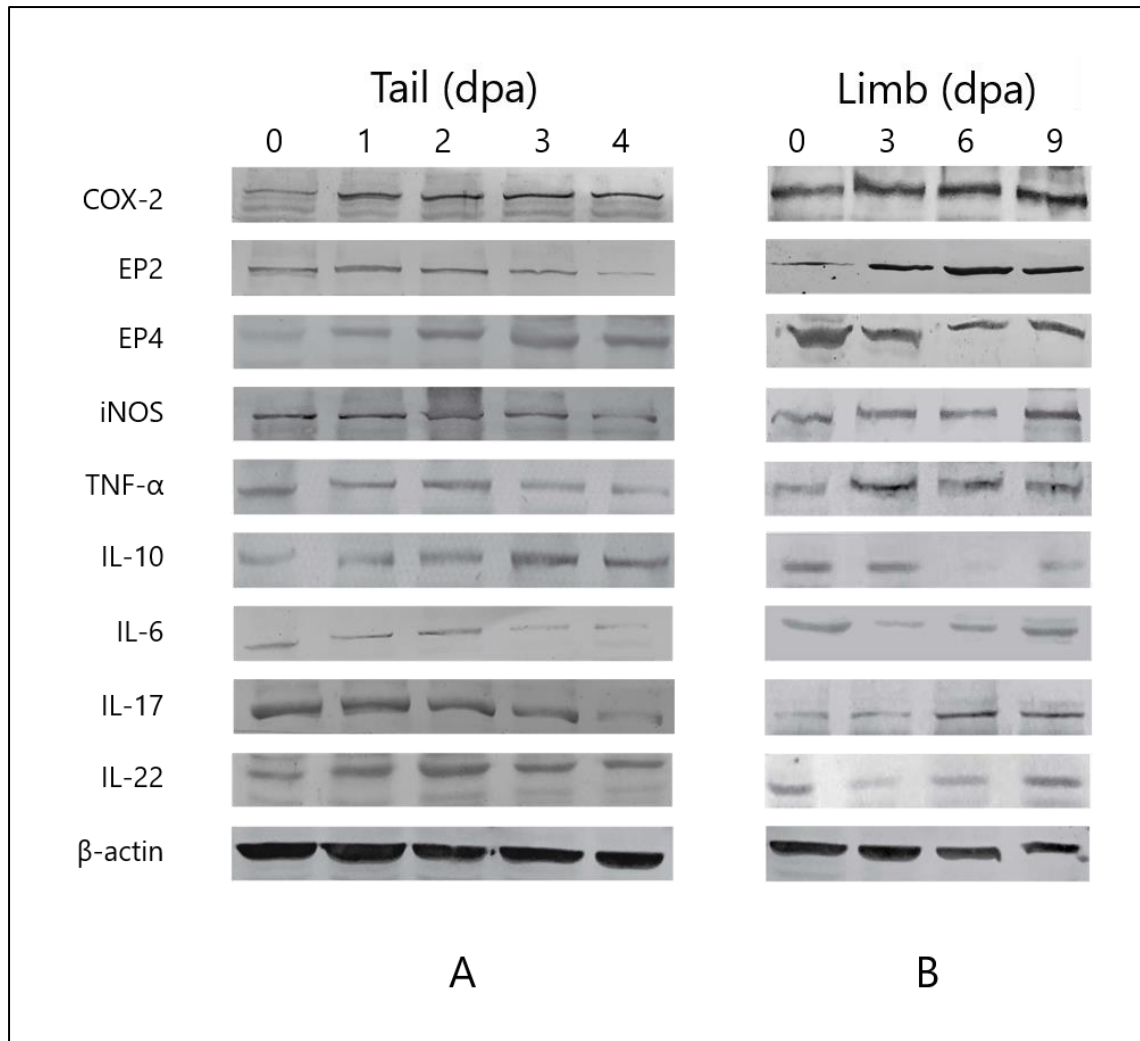
Figure 1.10: Western blot analysis in tail and limb

Western blot panel showing the band intensity during progressive wound healing for COX-2, EP2, EP4, iNOS, TNF-α, IL-10, IL-6, IL-17 and IL-22 proteins in both, healing tail and limb. β-actin was used as loading control.

Figure 1.11: q-RT-PCR analysis results in tail tissue

Gene expression analysis of inflammatory mediators in tail represented in fold change.
ns = not significant, *p ≤ 0.20, **p ≤ 0.005, ***p ≤ 0.001; n = 6

Figure 1.12: q-RT-PCR analysis results in limb tissue

Gene expression analysis of inflammatory mediators in limb represented in fold change. ns = not significant, *$p \leq 0.20$, **$p \leq 0.005$, ***$p \leq 0.001$; n = 6.

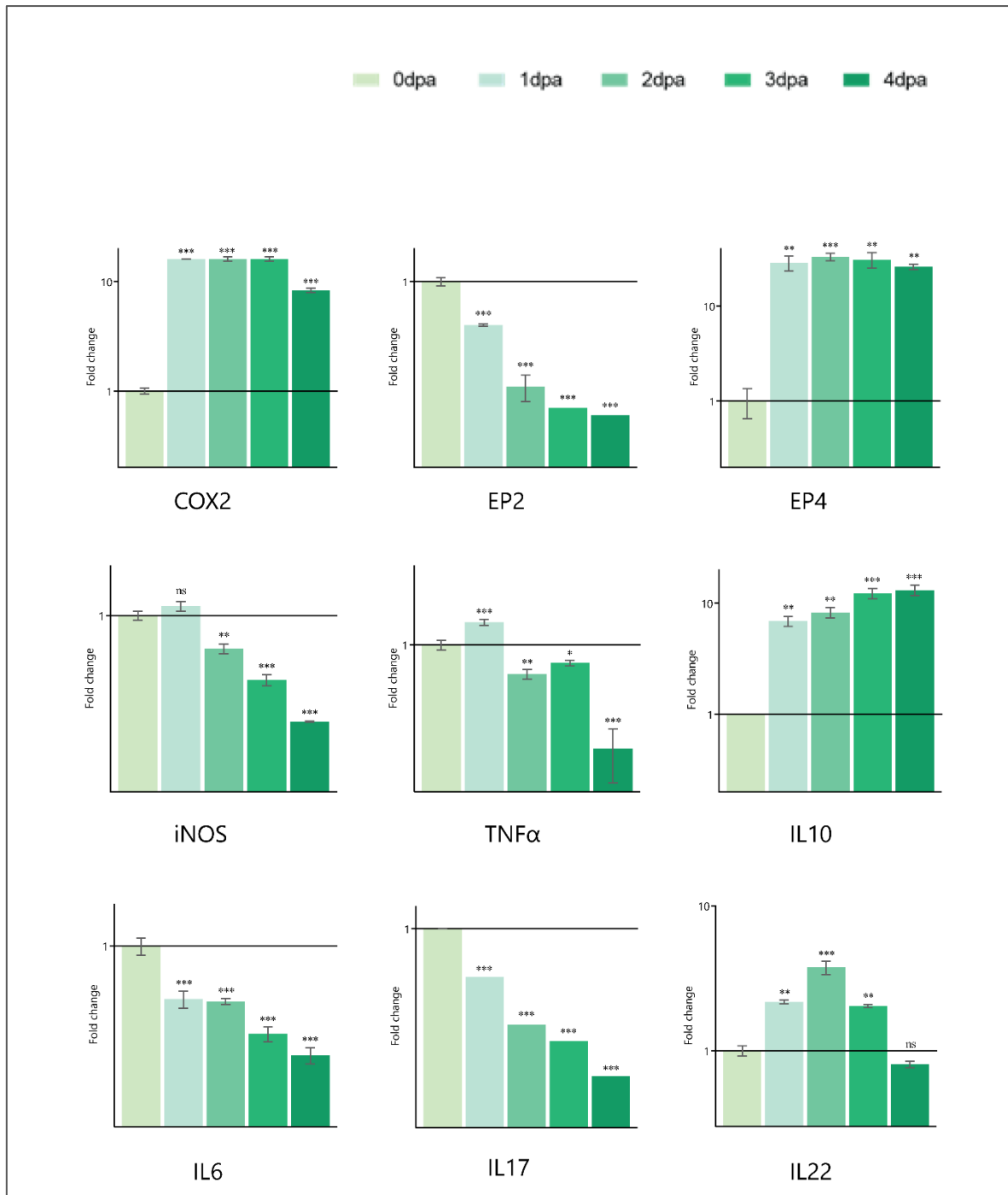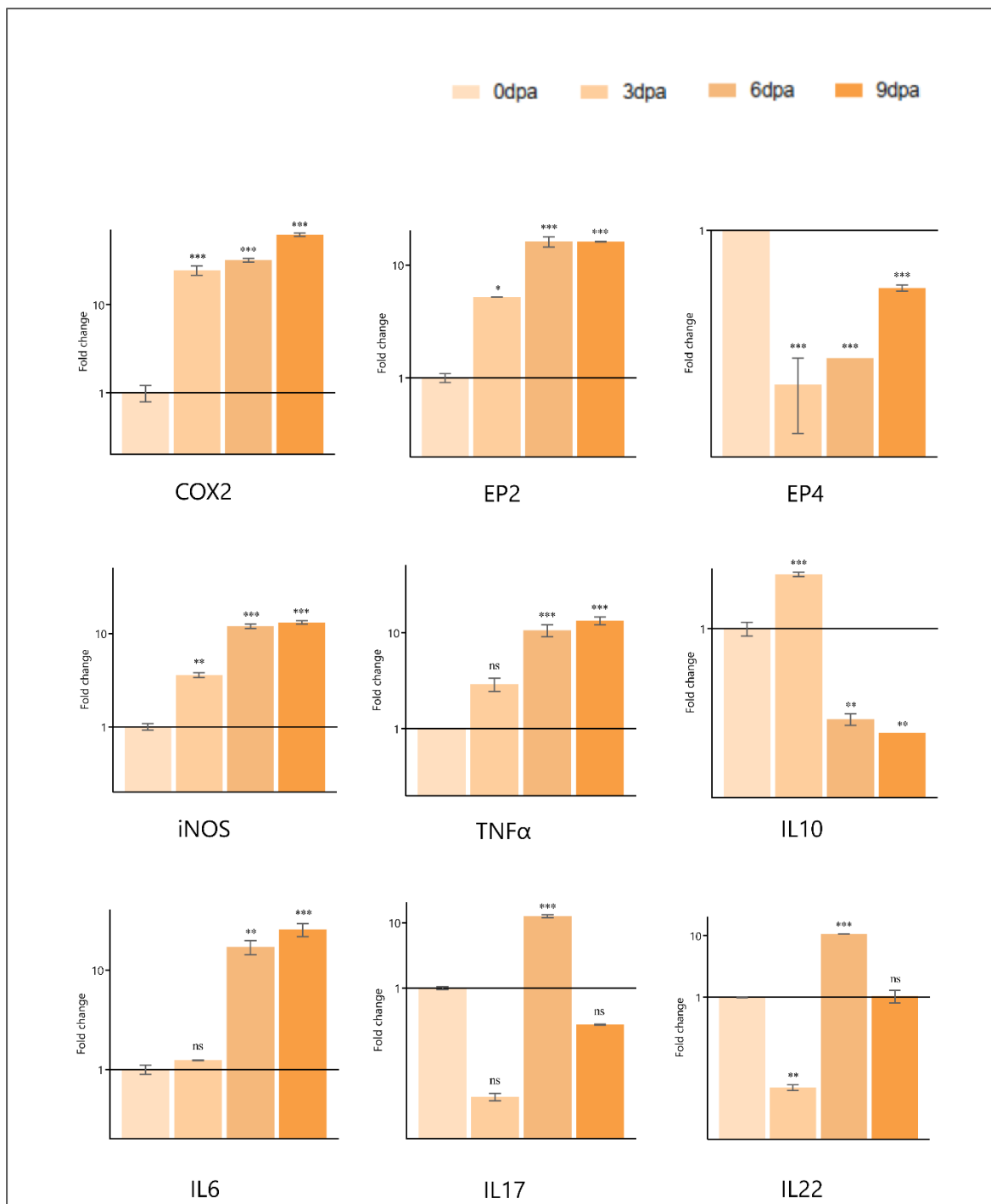| Gene	Forward (sequence 5'-3')	Reverse (sequence 5'-3')	NCBI ref. Id	Product length
COX-2	ACGTCTTACATCACGATCCC	GGAGAAGGCTTCCCAGCTTTT	NM_001167718.1	86
EP2	AGTTCAGCCAGAGCGAGAAC	AAGACCCAGGGGTCGATGAT	NM_001083365.1	85
EP4	CATTCCTCTGGTGGTCCGTG	GCTTGCAGGTCAGGGTTTTG	NM_001081503.1	87
iNOS	AACATGCTCCTTGAGGTGGG	CAGCTCGGTCCTTCCACAAT	NM_204961.1	184
TNF-α	GGGTGTTCGCGTTGTGATTT	TCTCACTGCATCGGCTTTGT	NM_001024447.1	171
IL-10	AAGGAGACGTTCGAGAAGATGG	TGATGAAGATGTCGAACTCCCC	NM_001004414.2	70
IL-6	TATCTATGAAGGCCGCTCCG	CCATTCCACCAACATTCGCC	XM_015281283.2	84
IL-17	ACAGGAGATCCTCGTCCTCC	CCTTTAAGCCTGGTGCTGGA	NM_204460.1	124
IL-22	AAGCGCTGAGTGCTGTAACT	CTTTTGGAGGTAGGGGGCTG	NM_001199614.1	150
18srRNA	GGCCGTTCTTAGTTGGTGGA	TCAATCTCGGGTGAAC	NR_003278.3	144

Table 1: List of primers used for qRT-PCR analysis

Proteins	Stages of wound healing				
	0dpa	1dpa	2dpa	3dpa	4dpa
COX-2	123 ± 1.60^a	150 ± 0.614^b	151 ± 1.35^b	144 ± 2.01^c	143 ± 1.30^c
EP2	92.9 ± 2.36^a	129 ± 1.92^b	140 ± 1.72^c	124 ± 2.59^b	118 ± 1.45^c
EP4	97.5 ± 1.18^a	113 ± 1.42^b	127 ± 1.38^c	125 ± 2.50^c	130 ± 1.15^c
iNOS	148 ± 1.36^a	148 ± 1.61^a	149 ± 1.82^a	135 ± 0.851^b	122 ± 1.35^c
TNF-α	120 ± 0.825^a	108 ± 2.21^b	130 ± 4.30^c	99.4 ± 1.07^d	89.9 ± 0.890^e
IL-10	94.1 ± 2.31^a	103 ± 1.34^b	106 ± 1.30^b	131 ± 3.08^c	122 ± 2.32^d
IL-6	110 ± 1.52^a	92.0 ± 3.39^b	106 ± 1.07^a	82.9 ± 1.89^c	82.8 ± 1.50^c
IL-17	151 ± 2.92^a	154 ± 1.86^a	144 ± 2.42^b	138 ± 3.00^b	123 ± 1.38^c
IL-22	111 ± 5.46^a	129 ± 2.97^b	140 ± 2.07^c	124 ± 2.94^b	132 ± 2.56^d
β-actin	227 ± 2.55^a	225 ± 2.98^a	219 ± 3.51^a	219 ± 2.90^a	205 ± 9.76^a

Table 2A: Band intensity (in arbitrary unit) of Western blot images of proteins in tail

Values are expressed as Mean ± SEM; Within each row, the values sharing the same superscript are not significantly different from each other; n = 6, from a pooled sample of 6 subjects; $p \leq 0.05$.

Gene	Forward (sequence 5'-3')	Reverse (sequence 5'-3')	NCBI ref. Id	Product length
COX-2	ACGTCTTACATCACGATCCC	GGAGAAGGCTTCCCAGCTTTT	NM_001167718.1	86
EP2	AGTTCAGCCAGAGCGAGAAC	AAGACCCAGGGGTCGATGAT	NM_001083365.1	85
EP4	CATTCCTCTGGTGGTCCGTG	GCTTGCAGGTCAGGGTTTTG	NM_001081503.1	87
iNOS	AACATGCTCCTTGAGGTGGG	CAGCTCGGTCCTTCCACAAT	NM_204961.1	184
TNF-α	GGGTGTTCGCGTTGTGATTT	TCTCACTGCATCGGCTTTGT	NM_001024447.1	171
IL-10	AAGGAGACGTTCGAGAAGATGG	TGATGAAGATGTCGAACTCCCC	NM_001004414.2	70
IL-6	TATCTATGAAGGCCGCTCCG	CCATTCCACCAACATTCGCC	XM_015281283.2	84
IL-17	ACAGGAGATCCTCGTCCTCC	CCTTTAAGCCTGGTGCTGGA	NM_204460.1	124
IL-22	AAGCGCTGAGTGCTGTAACT	CTTTTGGAGGTAGGGGGCTG	NM_001199614.1	150
18srRNA	GGCCGTTCTTAGTTGGTGGA	TCAATCTCGGGTGAAC	NR_003278.3	144

Table 1: List of primers used for qRT-PCR analysis

Proteins	Stages of wound healing				
	0dpa	1dpa	2dpa	3dpa	4dpa
COX-2	123 ± 1.60^a	150 ± 0.614^b	151 ± 1.35^b	144 ± 2.01^c	143 ± 1.30^c
EP2	92.9 ± 2.36^a	129 ± 1.92^b	140 ± 1.72^c	124 ± 2.59^b	118 ± 1.45^c
EP4	97.5 ± 1.18^a	113 ± 1.42^b	127 ± 1.38^c	125 ± 2.50^c	130 ± 1.15^c
iNOS	148 ± 1.36^a	148 ± 1.61^a	149 ± 1.82^a	135 ± 0.851^b	122 ± 1.35^c
TNF-α	120 ± 0.825^a	108 ± 2.21^b	130 ± 4.30^c	99.4 ± 1.07^d	89.9 ± 0.890^e
IL-10	94.1 ± 2.31^a	103 ± 1.34^b	106 ± 1.30^b	131 ± 3.08^c	122 ± 2.32^d
IL-6	110 ± 1.52^a	92.0 ± 3.39^b	106 ± 1.07^a	82.9 ± 1.89^c	82.8 ± 1.50^c
IL-17	151 ± 2.92^a	154 ± 1.86^a	144 ± 2.42^b	138 ± 3.00^b	123 ± 1.38^c
IL-22	111 ± 5.46^a	129 ± 2.97^b	140 ± 2.07^c	124 ± 2.94^b	132 ± 2.56^d
β-actin	227 ± 2.55^a	225 ± 2.98^a	219 ± 3.51^a	219 ± 2.90^a	205 ± 9.76^a

Table 2A: Band intensity (in arbitrary unit) of Western blot images of proteins in tail

Values are expressed as Mean ± SEM; Within each row, the values sharing the same superscript are not significantly different from each other; n = 6, from a pooled sample of 6 subjects; $p \leq 0.05$.

Proteins	Stages of wound healing			
	0dpa	**3dpa**	**6dpa**	**9dpa**
COX-2	149 ± 3.96^a	163 ± 2.27^b	169 ± 3.26^b	163 ± 2.09^b
EP2	179 ± 2.03^a	208 ± 3.47^b	203 ± 1.77^b	209 ± 0.667^b
EP4	154 ± 2.45^a	144 ± 1.31^b	140 ± 1.06^b	120 ± 1.24^c
iNOS	108 ± 1.65^a	115 ± 1.99^b	106 ± 1.41^a	139 ± 4.96^c
TNF-α	92.3 ± 2.04^a	158 ± 1.41^b	136 ± 1.89^c	130 ± 1.18^d
IL-10	111 ± 1.35^a	102 ± 1.41^b	58.4 ± 6.68^c	82.8 ± 1.35^d
IL-6	96.6 ± 2.37^a	75.5 ± 1.67^b	85.6 ± 1.48^c	104 ± 2.50^d
IL-17	86.4 ± 3.03^a	83.6 ± 2.52^a	119 ± 1.88^b	126 ± 2.42^c
IL-22	87.1 ± 3.75^a	53.7 ± 2.06^b	67.4 ± 2.57^c	106 ± 4.13^d
β-actin	214 ± 7.64^a	216 ± 8.45^a	207 ± 10.6^a	202 ± 9.90^a

Table 2B: Band intensity (in arbitrary unit) of Western blot images of proteins of limb

Values are expressed as Mean $\pm$ SEM; Within each row, the values sharing the same superscript are not significantly different from each other; n = 6, from a pooled sample of 6 subjects; $p \leq 0.05$.

Genes	Stages of wound healing				
	0dpa	**1dpa**	**2dpa**	**3dpa**	**4dpa**
COX-2	1 ± 0.06^a	16.10 ± 0.06^b	16.11 ± 0.70^b	16.11 ± 0.68^b	8.35 ± 0.37^c
EP2	1 ± 0.05^a	0.40 ± 0.01^b	0.11 ± 0.03^b	0.07 ± 0.00^c	0.06 ± 0.00^d
EP4	1 ± 0.20^a	28.5 ± 1.28^b	32.9 ± 1.72^b	30.70 ± 1.58^b	25.80 ± 0.91^c
iNOS	1 ± 0.57^a	1.23 ± 0.07^a	0.48 ± 0.03^b	0.24 ± 0.03^c	0.10 ± 0.00^d
TNF-α	1 ± 0.05^a	1.59 ± 0.05^a	0.5 ± 0.03^b	0.69 ± 0.02^b	0.12 ± 0.03^c
IL-10	1 ± 0.00^a	6.89 ± 0.30^b	8.25 ± 0.45^c	12.25 ± 0.63^d	13.1 ± 0.58^d
IL-6	1 ± 0.08^a	0.41 ± 0.01^b	0.40 ± 0.01^b	0.23 ± 0.00^c	0.16 ± 0.01^d
IL-17	1 ± 0.07^a	0.22 ± 0.00^b	0.05 ± 0.00^c	0.03 ± 0.00^d	0.01 ± 0.00^e
IL-22	1 ± 0.008^a	2.17 ± 0.07^b	3.76 ± 0.18^c	2.03 ± 0.00^b	0.80 ± 0.04^d

Table 3A: Fold change in the expression of genes at different healing stages in tail

Values are expressed as Mean $\pm$ SEM; Within each row, the values sharing the same superscript are not significantly different from each other; n = 3, from a pooled sample of 6 subjects; $p \leq 0.05$.

Genes	Stages of wound healing			
	0dpa	3dpa	6dpa	9dpa
COX-2	1 ± 0.12^a	24.58 ± 1.37^b	31.0 ± 1.66^c	62.20 ± 2.89^d
EP2	1 ± 0.05^a	5.20 ± 0.02^b	16.11 ± 1.67^c	16.07 ± 0.00^c
EP4	1 ± 0.00^a	0.37 ± 0.02^a	0.11 ± 0.00^b	0.07 ± 0.00^b
iNOS	1 ± 0.08^a	3.58 ± 0.22^b	12.0 ± 0.66^c	13.12 ± 0.57^c
TNF-α	1 ± 0.00^a	2.90 ± 0.20^b	10.00 ± 0.66^c	13.30 ± 0.57^d
IL-10	1 ± 0.16^a	3.51 ± 0.15^b	0.12 ± 0.00^c	$0.09 \pm 0.00c$
IL-6	1 ± 0.11^a	1.23 ± 0.00^a	17.03 ± 0.86^c	25.58 ± 1.15^d
IL-17	1 ± 0.06^a	0.02 ± 0.00^b	12.00 ± 0.63^c	0.28 ± 0.00^d
IL-22	1 ± 0.00^a	0.03 ± 0.00^b	10.00 ± 0.05^c	1.05 ± 0.08^a

Table 3B: Fold change in the expression of genes at different healing stages in limbs

Values are expressed as Mean ± SEM; Within each row, the values sharing the same superscript are not significantly different from each other; n = 3, from a pooled sample of 6 subjects; $p \leq 0.05$.

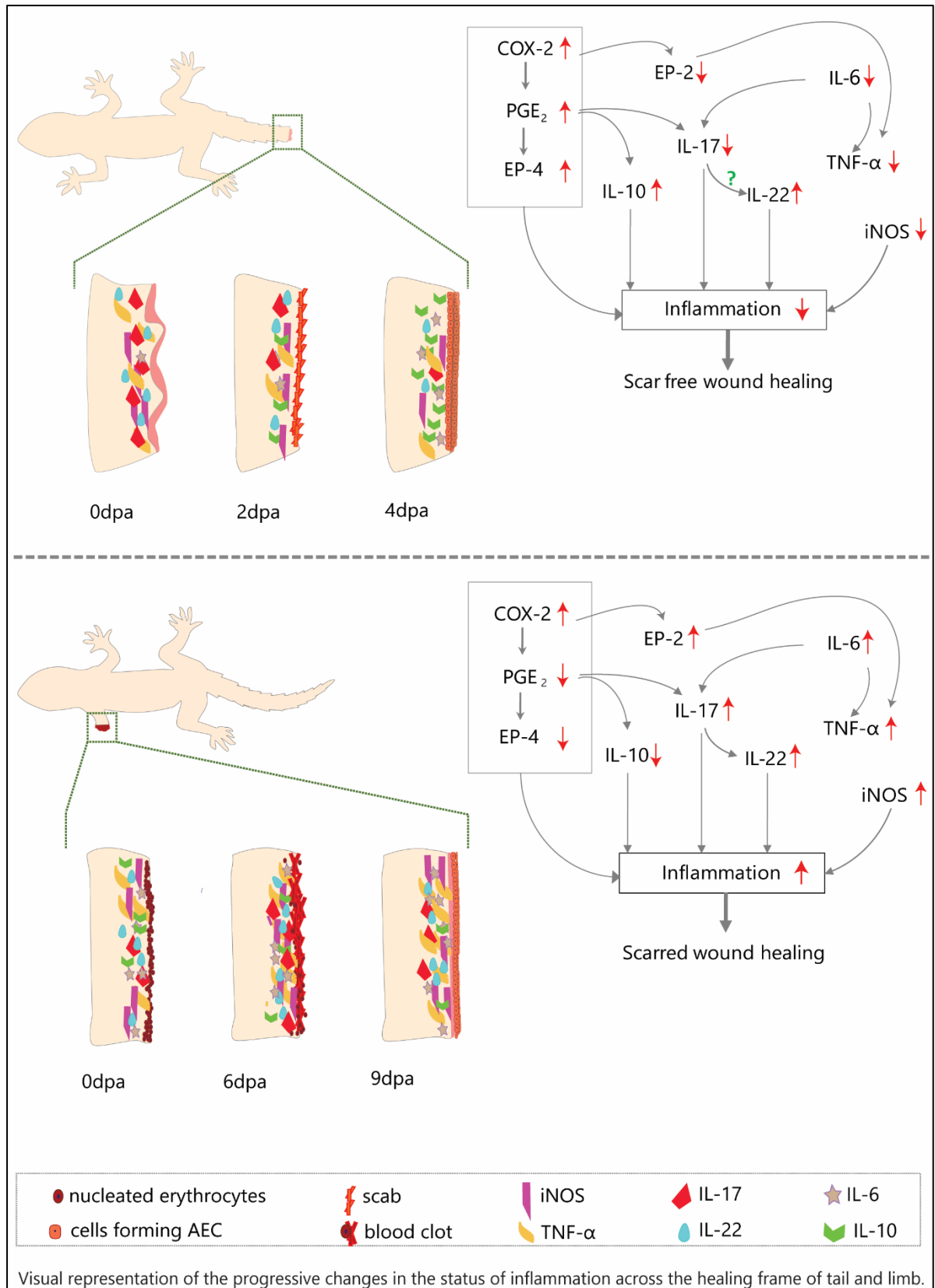Visual representation of the progressive changes in the status of inflammation across the healing frame of tail and limb.

Figure 1.13 Chapter Summary